Cement and Concrete Research 40 (2010) 488–496

Contents lists available at ScienceDirect

Cement and Concrete Research

journal homepage: http://ees.elsevier.com/CEMCON/default.asp

High temperature behaviour of self-consolidating concrete Microstructure and physicochemical properties

Hanaa Fares *, Sébastien Remond, Albert Noumowe, Annelise Cousture

L2MGC, Université de Cergy-Pontoise, F-95000 Cergy-Pontoise, France

ARTICLE INFO

Article history:
Received 27 May 2009
Accepted 5 October 2009

Keywords:
Self-consolidating concrete
Temperature (A)
SEM (B)
Image analysis (B)
Physical properties (C)

ABSTRACT

This paper presents an experimental study on the properties of self-compacting concrete (SCC) subjected to high temperature. Two SCC mixtures and one vibrated concrete mixture were tested. These concrete mixtures come from the French National Project B@P. The specimens of each concrete mixture were heated at a rate of 1 °C/min up to different temperatures (150, 300, 450 and 600 °C). In order to ensure a uniform temperature throughout the specimens, the temperature was held constant at the maximum temperature for 1 h before cooling. Mechanical properties at ambient temperature and residual mechanical properties after heating have already been determined. In this paper, the physicochemical properties and the microstuctural characteristics are presented. Thermogravimetric analysis, thermodifferential analysis, X-ray diffraction and SEM observations were used. The aim of these studies was in particular to explain the observed residual compressive strength increase between 150 and 300 °C.

1. Introduction

The use of self-consolidating concrete (SCC) has considerably developed during the last years and a growing attention has been brought to the study of its mechanical properties at hardened state. The mixture proportions of SCC (large paste volume, high content of mineral admixtures, coarse to fine aggregates ratio close to 1, …) in relation with its placing conditions could modify its mechanical behaviour, comparatively to traditional vibrated concrete. The behaviour of SCC subjected to high temperature has in particular to be evaluated.

In case of fire, concrete is exposed to high temperature that induces a material degradation: strength decrease, cracking, and in some conditions spalling. Up to now, the effect of elevated temperature has been studied mainly on vibrated ordinary and high performance concretes. The few studies on SCC subjected to high temperature showed either a decrease in strength or an increase in the risk of spalling [1–3], or a behaviour similar to that of vibrated concrete [4–6].

The aim of this study is to analyze the behaviour of SCC subjected to high temperature. Three mixes were investigated: two SCC and one Vibrated Concrete (VC). The residual mechanical strength and physical properties have already been studied [7]. The observed mechanical behaviours are explained through the microstructure and the physicochemical properties of these concretes.

2. Materials and concrete mixes

The three studied mixes investigated in our research work are presented in Table 1. These concrete mixes have been developed for the French National Project B@P [8].

With these concretes, cylindrical specimens 16 × 32 cm and prismatic specimens 10 × 10 × 40 cm were prepared. After molding, the specimens were covered by a plastic sheet and cured at ambient temperature during 7 days before being removed from the mould and sealed in watertight bags for storage at ambient temperature. The mechanical tests were carried out, according to the RILEM recommendations [9], after curing for more than 90 days.

Table 1
Concrete mixes.

1 m^3	SCC 1	SCC 2	VC
CEM I 52.5 N	–	350	373
CEM II 32.5 R	328	–	–
Limestone Filler	225	130	–
Sand 0/4	795	857	913
Aggregates 4/22.5	745	742	790
Water	199	200	202
Slump (cm)	65	71	19
Water/Cement	0.61	0.57	0.54
Water/Powder	0.36	0.42	0.54
Strength at 90 days (MPa)	37	54	41

* Corresponding author.
E-mail address: hanaafares@yahoo.fr (H. Fares).

0008-8846/$ – see front matter © 2009 Elsevier Ltd. All rights reserved.
doi:10.1016/j.cemconres.2009.10.006

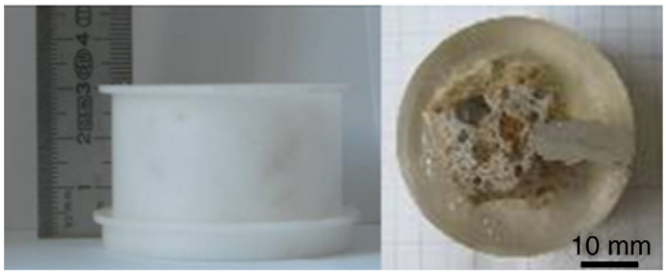

Fig. 1. Mould and specimen for SEM observations.

3. Tests

3.1. Test temperature

The specimens were subjected to four different temperature cycles from 20 °C up to 150, 300, 450 and 600 °C. The first part of each cycle consisted of a heating at 1 °C/min up to the target temperature. After what, the temperature was held constant for 1 h in order to ensure an uniform temperature throughout the specimens. The last part of the cycles consisted of a cooling down to ambient temperature. The rate of heating refers to the recommendations of the RILEM Technical Committee TC-129 [9].

3.2. Microscopic observations (SEM — Scanning electron microscopy)

Mechanical tests were performed at ambient temperature and after exposure to high temperature in order to determine the residual compressive strength, flexural strength and modulus of elasticity. All these results have been presented in a previous paper [7]. After each mechanical test, concrete samples were taken and put in plastic bags in order to carry out physicochemical characterizations and microscopic observations. Abrasive wet-cutting was used in order to prevent damaging the samples. Samples of 3 or 4 cm have been drilled out concrete without coarse aggregates.

After wet-cutting, the samples used for the SEM observations were dried at 50 °C, and then coated in cold epoxy resin (Fig. 1).

When the resin was hardened, the samples could be polished according to the following procedure. First, the samples were ground with abrasive paper SiC p220, p500, p800 and p1200 (respectively 70, 30, 22 and 15 μm). Then, they were polished with diamond pastes of decreasing diameter (6, 3, and 1 μm) during 2 min for each paste. In

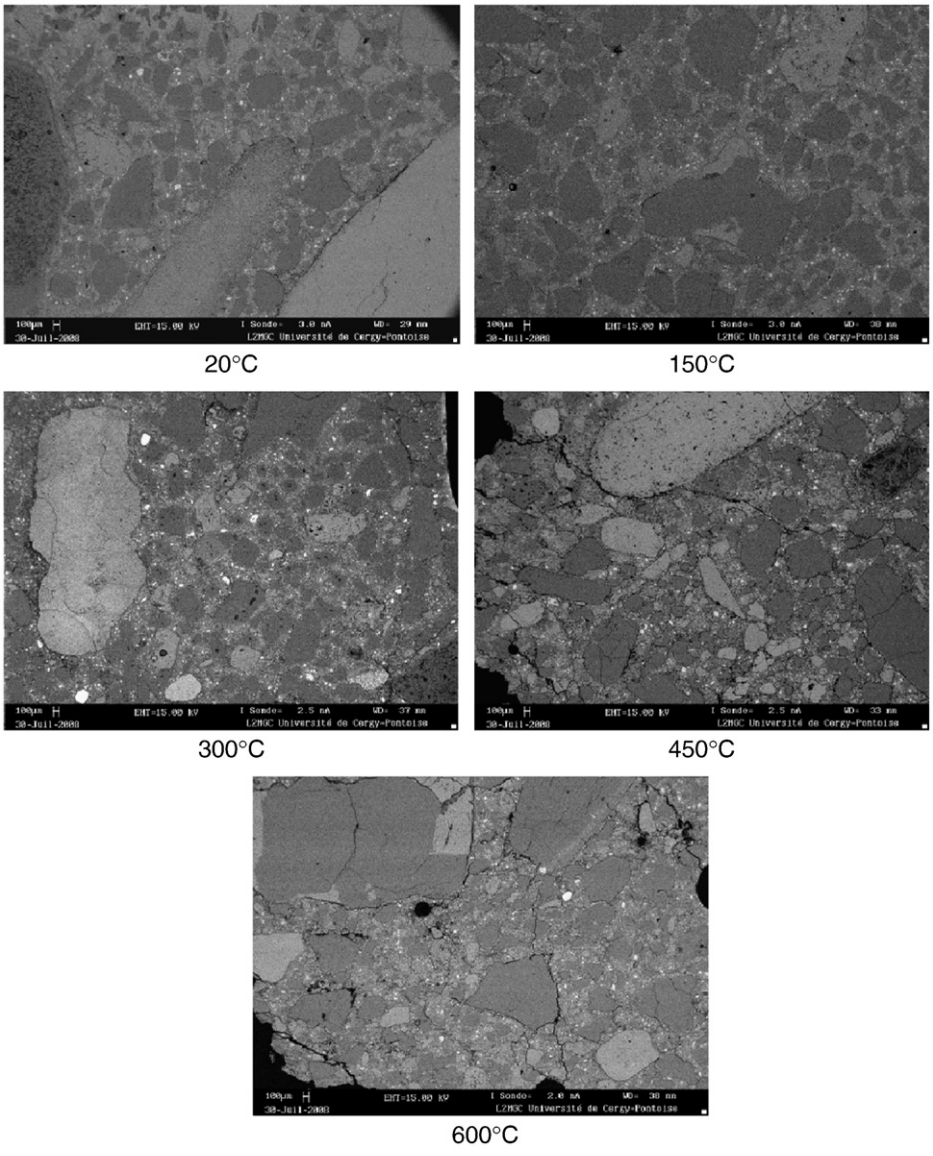

Fig. 2. SEM images of SCC 2 after exposure to high temperature.

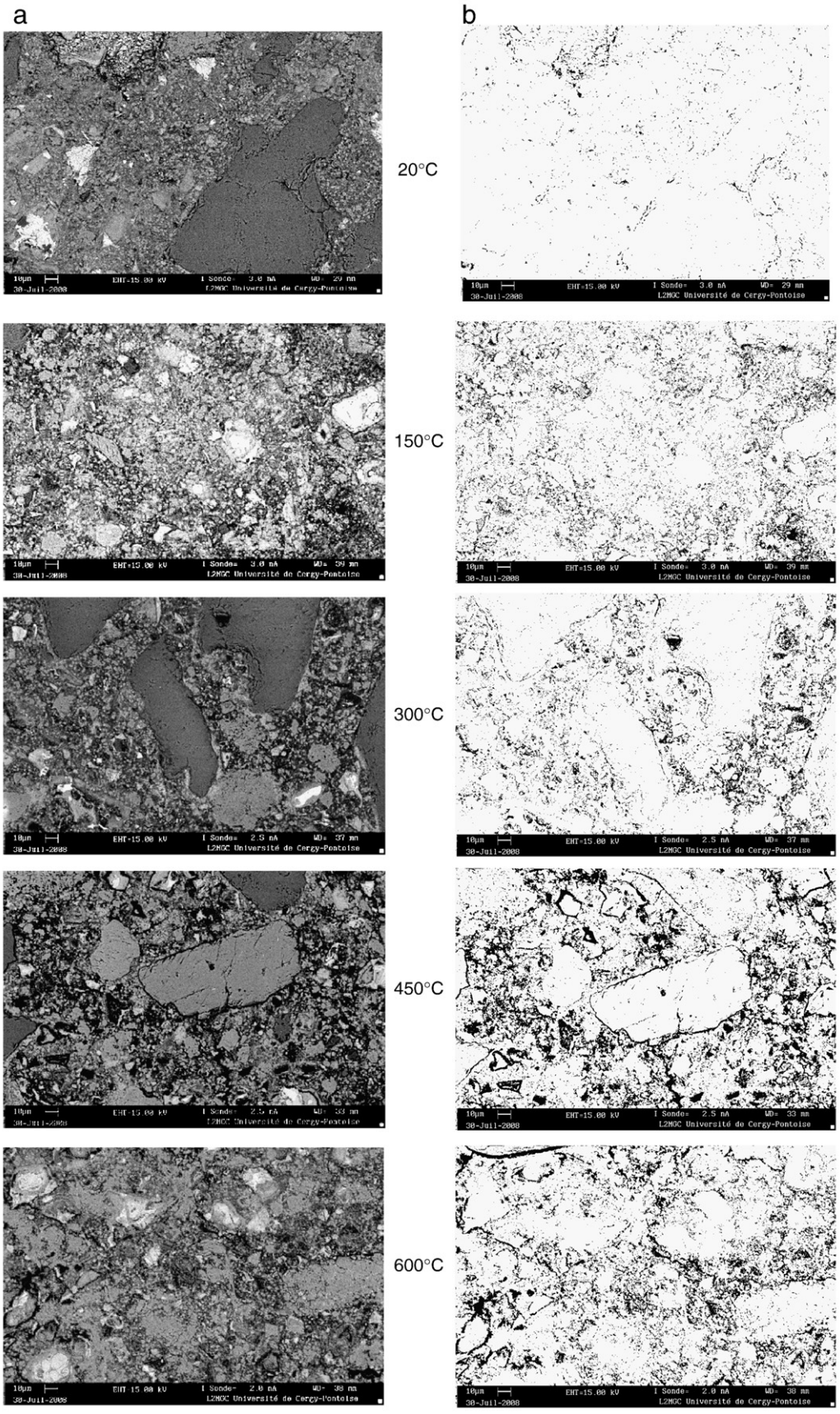

Fig. 3. SEM images (a) and porosity images obtained after image analysis (b) (SCC 2).

order to remove any residual polishing compound, a cleaning with ethanol was carried out [10]. The samples were coated with nickel to provide a conductive surface for SEM observations. A Scanning Electron Microscopy LEICA S430i was used.

The observations have been carried out with backscattered electrons signal (BEI), which allows an important chemical contrast. This contrast depends on the average atomic number of the observed phases, the clearest phases corresponding to the largest average atomic number [11]. Anhydrous cement appears brightest followed by calcium hydroxide, calcium silicate hydrate, and aggregates. Voids appear dark [11].

3.3. Image analysis

In order to quantify the porosity and the fraction of anhydrous elements of the different concretes, image analyses have been carried out on each sample. Twenty pictures have been collected with a magnification 800× (approximate size 285 μm × 215 μm). Before image analysis, brightness and contrast are fitted to obtain all grey level values between 0 and 256 [12,13].

The pictures have been analyzed using the free software "Image J" initially developed by the Research Services Branch (RSB) of National Institute of Health [14]. On each picture, after erasing the aggregates, a grey level threshold is defined allowing to show either the porosity or the anhydrous phases. The porosity and the proportion of anhydrous elements can be determined on each picture using the surface fraction area of each studied phase [15].

3.4. DTA–TGA

Thermogravimetric (TGA) and differential thermal analyses (DTA) have been carried out by using a SETARAM Labsys 1200. DTA determines the heat flow of materials subjected to a heating. Mortar samples were taken from concrete specimens subjected to high temperature and stored in watertight bags. Then, they were crushed in powder and kept in hermetic flasks. Each sample was submitted to a heating at a rate of 20 °C/min up to 800 °C under argon atmosphere. The measure of the heat flow allows to determine the temperature where phase changes take place [16].

Thermogravimetric analysis consists of measuring the mass variation during heating and allows to determine the phase changes.

3.5. X-ray diffraction

In order to identify the crystal phases in the different samples, X-ray diffraction analysis (using copper Kα radiation) have been conducted. Samples were prepared the same way as for DTA.

4. Results and discussion

4.1. Microscopic observations (SEM)

Fig. 2 presents SEM images obtained on SCC 2 at ambient temperature and after exposure to high temperature (approximate size 7315 μm × 5485 μm, magnification X30).

Up to 150 °C, the surface of the observed concrete did not present any features of deterioration. No visible cracking could be distinguished.

At 300 °C, few cracks appeared, notably in the interfacial transition zone between aggregates and paste. The cracks aspect was more pronounced for the samples heated to 450 °C and especially to 600 °C. At these temperatures, many cracks could be observed in the interfacial transition zone between aggregates and paste, but also in the paste and aggregates, notably at 600 °C. These cracks through aggregates observed at this temperature certainly result from the presence of quartz (SiO_2) in the aggregates. Indeed, towards 570 °C, the allotropic transformation of quartz-α in quartz-β occurred. This reversible transformation had important effects on the physical properties of quartz and induced in particular an expansion (0.8% in volume). These observations could be done on each concrete. Similar cracks appeared at the same temperatures for all the concretes.

4.2. Image analysis

Fig. 3a) and b) present the images obtained with SEM and the images resulting from image analysis and showing the porosity of SCC 2.

An important increase in porosity with the increase in temperature was observed. Between 20 and 600 °C, the porosity increases by a factor of two. It was not only due to the cracking of samples but also to the deterioration of the cement paste with the departure of bound water. Liu et al. [17–19] also observed an important increase in porosity on SCC and HPC subjected to elevated temperature. Moreover, they observed that pore size and shape are significantly influenced by temperature. At 130 °C, porosity is lower and pores are more irregular than those observed at 400 °C. They report that up to 500 °C, the main physicochemical changes are the loss of water and the decomposition of calcium hydroxide. These transformations induce the collapse of the gel structure and create additional porosity by the alteration of the porous media: they observed an increase in porosity by a factor of 1.5 between 400 and 500 °C. In our study, the increase corresponds to a factor of 1.4 (in average) between 20 and 450 °C.

Fig. 4 presents a comparison between water porosity obtained experimentally [7] and porosity measured by image analysis as a function of temperature. The evolutions obtained by the two experimental methods were similar for each concrete mix. The porosity obtained by image analysis had the same order of magnitude, but was generally lower than the water porosity. The difference was certainly linked to a better accessibility of the pores of small size by water in comparison to the resin. Moreover, the SEM observations didn't allow obtaining a sufficiently fine resolution to quantify the finest porosity. The evolution of the porosity was monotonous and increased with the temperature [2,3,20].

Fig. 5a) presents the same BEI than those shown in Fig. 3a). Fig. 5b) presents the results of the image analysis in which the clearest phases (in black on Fig. 5b) have been separated from the other ones.

Fig. 6 presents the variations of the surface fraction of the clearest phases observed for each concrete as a function of the temperature. The surface fraction of the clearest phases for the two SCC decreased between 20 and 300 °C then increased monotonly above 300 °C. This fraction increased monotonly with the temperature between 20 and 600 °C for the vibrated concrete.

Between 20 and 300 °C, the clearest phases on BEI corresponded essentially to the anhydrous phases of the cement (Fig. 5). Up to

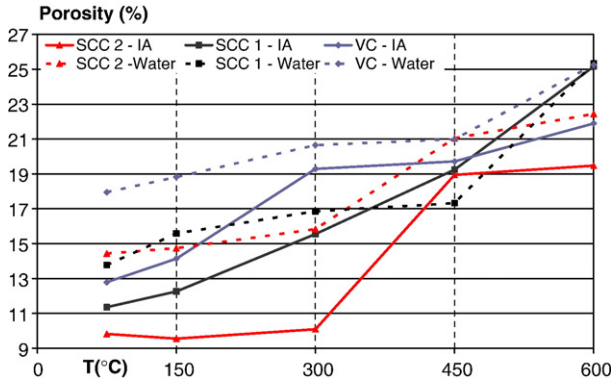

Fig. 4. Evolution of water porosity [7] and porosity obtained by image analysis (IA).

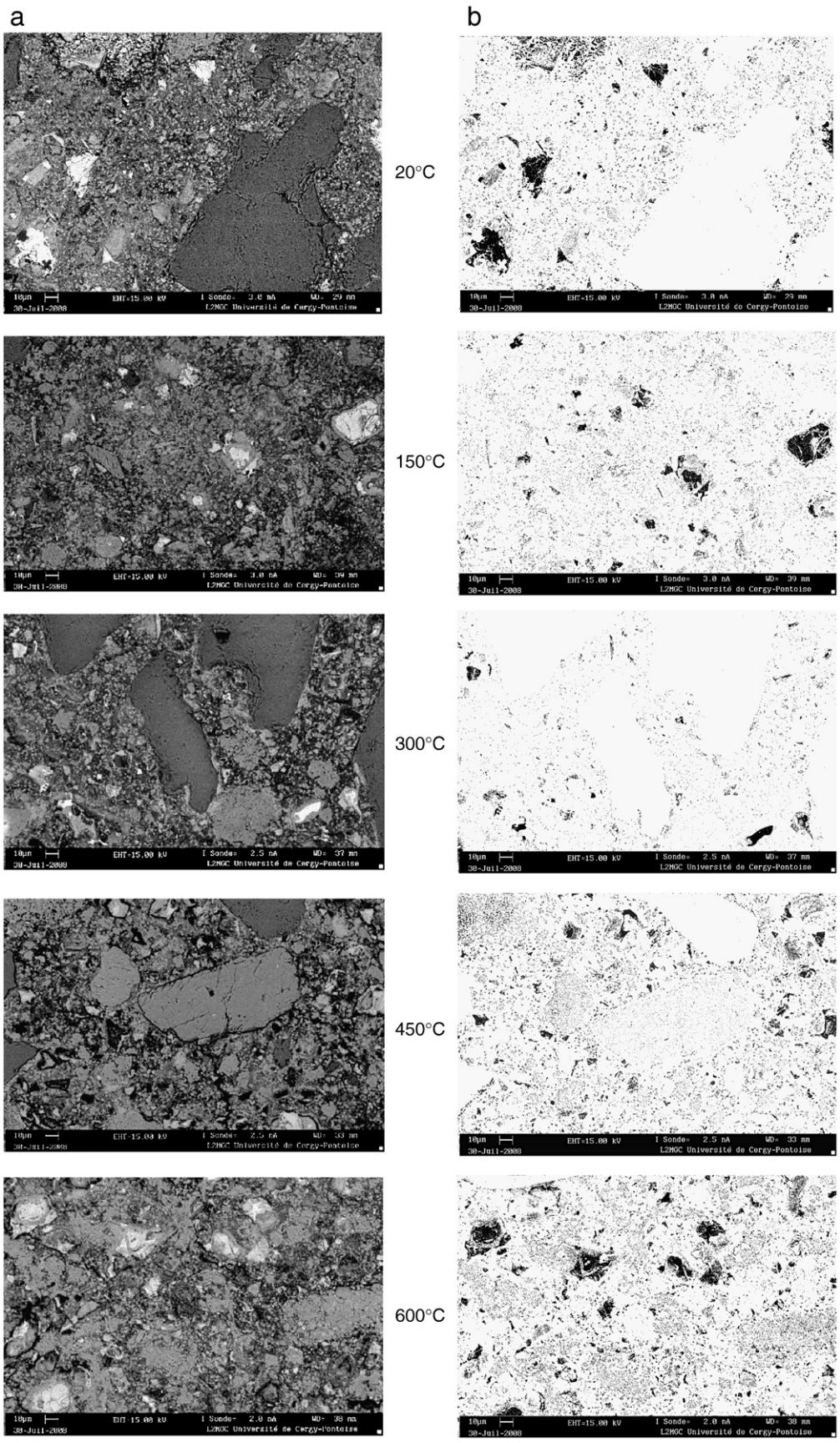

Fig. 5. SEM images (a) and anhydrous phases images (b) as function of temperature (SCC 2).

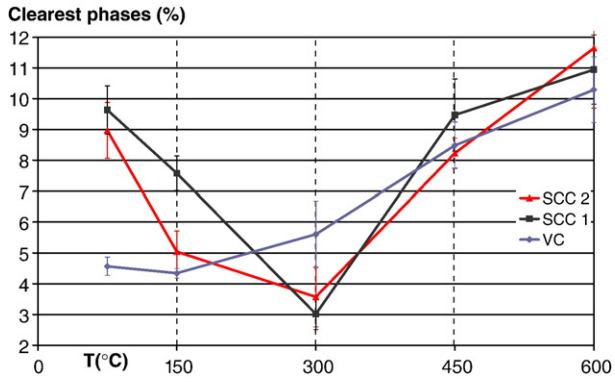

Fig. 6. Evolution of the surface fraction of the clearest phases on the BE images as a function of the temperature.

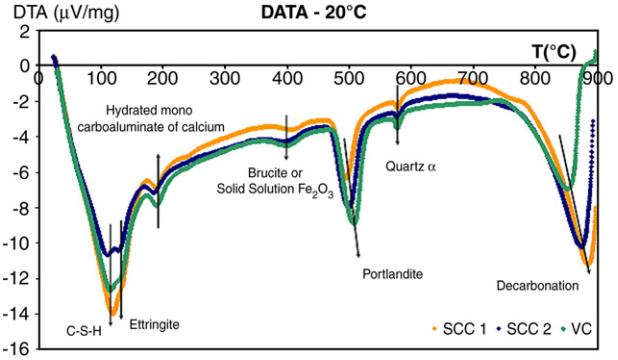

Fig. 8. Differential thermal analysis of unheated concretes.

300 °C, there was a supplementary hydration of anhydrous cement, due to the important water movements that were produced during the heating between 100 and 300 °C. The water movements were due, on the one hand, to the departure of free water (up to about 150 °C) [21] and on the other hand to the departure of bound water coming from the dehydration of C–S–H. This later created an increase in the porosity of C–S–H, as seen in SEM observations and allowed probably water to attain the anhydrous grains of cement. At 300 °C, all the anhydrous grains of cement have been rehydrated.

Above 300 °C, we observed an increase in the surface fraction of the clearest phases. These phases certainly didn't correspond anymore to anhydrous phases, but doubtless to dense phases coming from the decomposition of hydrates. These phases become difficult to identify, indeed, according to Liu et al. [19], when the samples are heated up to 400 °C the brightness of several phases become too close to be distinguished.

The evolution of the surface fraction of anhydrous phases allowed explaining the results concerning the compressive strength behaviour of concretes exposed to high temperature [7]. These results are recalled in Fig. 7 presenting the evolution of residual compressive strength as a function of the temperature for the three studied concretes.

The behaviour of SCC and vibrated concrete differs significantly between 20 and 300 °C. On the one hand, for the two SCC, after a moderate decrease in compressive strength between 20° and 150 °C, an important increase (about 25%) is observed between 150 and 300 °C. On the other hand, for the vibrated concrete (VC), the relative compressive strength decreases monotonly. However, the decrease observed between 150 and 300 °C for VC is moderate (about 5%). Given the large standard deviation observed for this concrete, this result cannot be generalized. Beyond 300 °C, an important decrease in strength is observed for all the mixes.

Several hypotheses have been proposed in the literature to explain this increase in strength. Dias et al. [22] attributed the increase in the residual compressive strength between 150 and 300 °C to a rehydration of the paste due to the migration of water in the pores. In another study, Khoury [23] assumes that the silanols groups lose a part of their bonds with water, which induces the creation of shorter and stronger siloxane elements (Si–O–Si) with probably larger surface energies that contribute to the increase in strength.

Our results clearly show that the evolution of residual compressive strength between 150 and 300 °C is strongly correlated to the evolution of anhydrous cement. The compressive strength of the two SCC increases together with a decrease in the amount of anhydrous cement. On the contrary, no further hydration is observed for the VC while its compressive strength decreases. These results confirm the hypothesis of Dias et al [22]. However, it has to be pointed out that the porosity of all the concrete mixes increases between 150 and 300 °C. The increase in compressive strength of the two SCC between 150 and 300 °C is therefore not due to a filling of the porosity by new hydration products. These new hydration products are certainly formed, but their volume is not large enough to compensate the increase in porosity due to cracking and to the dehydration of C–S–H. Dias hypothesis is not sufficient to explain the evolution of compressive strength. The increase in strength is therefore also due to an increase in the bonding properties of hydrates (a larger compressive strength is obtained for a larger porosity of the material). We think that the two previous hypothesis [22,23] could be combined into the following: the increase in compressive strength between 150 and 300 °C is due to the hydration of anhydrous phases which leads to the formation of hydrates having better bonding properties.

Similar tests (images analysis) carried out by Liu [17] on SCC did not show this decrease in the fraction of anhydrous cement grains. Liu simply observed fluctuations that were related to the experimental dispersion of samples. However, he did not observe any increase in

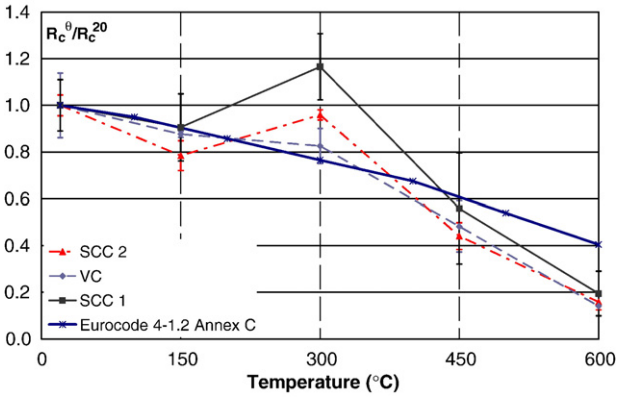

Fig. 7. Evolution of relative residual compressive strength with temperature.

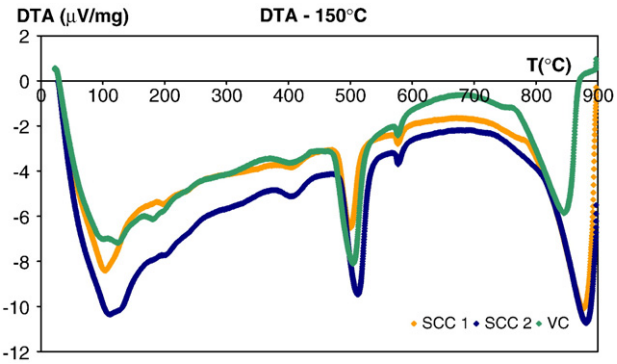

Fig. 9. DTA on concretes heated up to 150 °C.

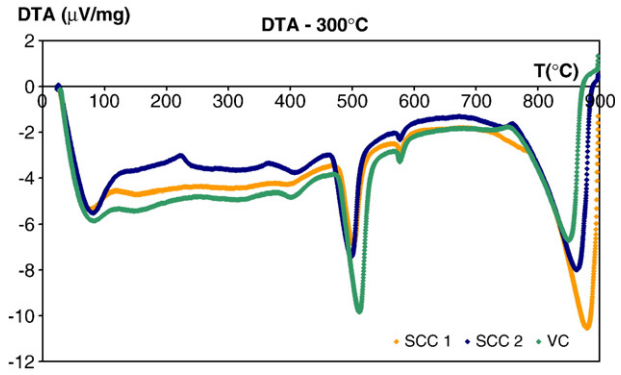

Fig. 10. DTA on concretes heated up to 300 °C.

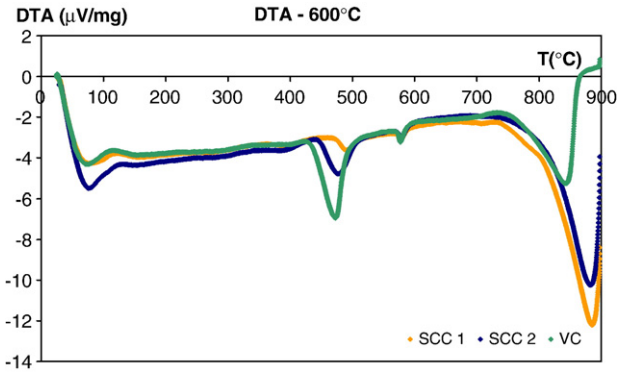

Fig. 12. DTA on concretes heated up to 600 °C.

compressive strength between 150 and 300 °C. His results are in agreement with the previous conclusion.

In order to specify the nature of the phases that decompose or form during the heating, X-ray diffraction analysis, DTA and TGA were carried out.

4.3. Thermogravimetric and differential thermal analysis

Fig. 8 presents differential thermal analysis (DTA) of unheated specimens (before thermal treatment). We observed 6 different endothermic peaks: 110–130 °C, 200 °C, 400 °C, 500 °C, 570 °C and 850 °C.

These different peaks of heat flow are linked to the temperatures of phase transition of the different hydrates in the cement paste.

The double peak at 110–130 °C can be attributed to the departure of water in some hydrates like C–S–H and ettringite [24,25]. At 200 °C, the presence of a peak indicates the dehydration of hydrated calcium monocarboaluminate [26].

Khoury [23], Noumowé [20], and Richard [27] attribute the slight variation of heat flow between 200 and 300 °C, to continuous dehydration of C–S–H. According to several authors [17,28], the variation of heat flow between 200 and 400 °C is due mainly to the loss of water from pores of hydrates as well as to the first stage of dehydration and breakdown of tobermorite gel.

A small peak can be observed around 400 °C. The phase that undergoes a modification at this temperature was not clearly identified. A similar transformation has been observed by Sha et al. [29] and by Persy et al. [24] on cement pastes. The first authors attributed this peak to the crystal change or to the dehydration of a solid solution of Fe_2O_3 [29]. On the contrary, Persy et al. [24] attributed it to the decomposition of brucite ($Mg(OH)_2$). We can only emit hypotheses on the nature of this phase.

Between 450 and 550 °C, the portlandite decomposes into free lime (dehydroxylation) [20,21,25].

At 573 °C, the allotropic transformation of quartz-α into quartz-β takes place with an expansion (cracking in siliceous aggregates) [21].

As Platret et al. [21], we observed that between 600 and 700 °C, C–S–H decomposes and forms β-C_2S.

Between 700 and 900 °C, the carbonate of calcium decomposes and CO_2 escapes from the concrete [20,23]. Ye et al. [28] compared SCC pastes with HPC pastes. SCC pastes showed a better stability below 700 °C due to low cement content in the mixtures. However, when the temperature was higher than 700 °C, a drastic mass loss was observed in the SCC pastes containing limestone filler due to their decarbonation. Indeed, our tested concrete present a high peak as a function of the limestone filler content: SCC had a peak clearly more marked than VC, like Ye et al. [28].

Figs. 9–12 present DTA results of heated concretes (heating at 1 °C/min). Comparatively to the Fig. 7, several peaks have disappeared, or are reduced, which corresponded to the partial or total decomposition of some phases during the thermal treatments.

After a heating up to 150 °C, the results are slightly modified in comparison to Fig. 8. In fact, the peak at 110–130 °C diminished because of the departure of free water and dehydration of the C–S–H and ettringite [20,25].

After heating up to 300 °C, free water, bound water of C–S–H, ettringite and hydrated calcium monocarboaluminate have been eliminated.

Above 300 °C (comparatively to a heating to 300 °C), the peak at 400 °C disappeared. This result indicated the absence of the phase that could be the crystal phase Brucite or solid solution of Fe_2O_3 according to the authors [24,29].

For the heating to 600 °C, the peak at 500 °C diminished significantly in comparison to 20 °C. That corresponded to the dehydroxylation of portlandite. Furthermore, the peak at 573 °C corresponding to the allotropic transformation of the quartz-α in quartz-β remained unchanged. With this reversible transformation, we could suppose that quartz-α reformed after cooling, once the thermal treatment finished.

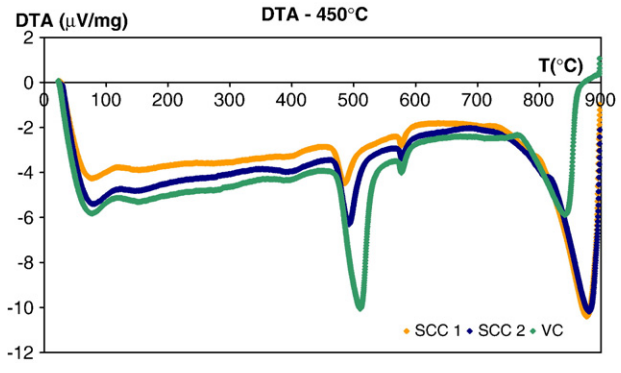

Fig. 11. DTA on concretes heated up to 450 °C.

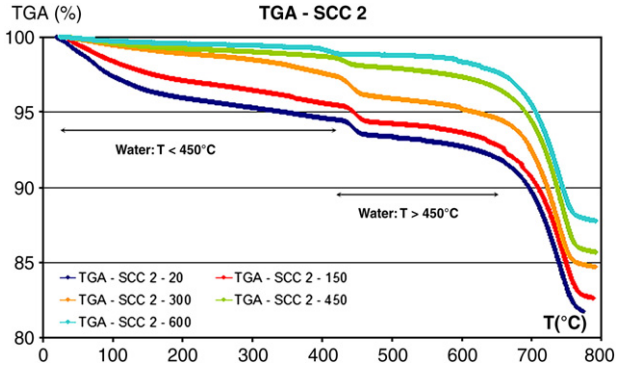

Fig. 13. TGA on SCC 2 for each tested temperature.

These results show that water in concrete (free water then bound water) was eliminated progressively according to his cohesion forces. The hydrates and the aggregates underwent transformations according to the nature of the minerals they contain. These physical and chemical transformations, in particular the departure of bound water, resulted in an important increase in the porosity of the concrete (Fig. 4), which then induced a change of the mechanical properties of the material as well as of its transfer properties. All these phenomena were similar for all the tested concretes and can be generalized.

Fig. 13 presents the results of the thermogravimetric analysis representing the mass variations of unheated and heated samples from 20 up to 800 °C for SCC 2. With the temperature elevation, the mass loss increased, then stabilized towards 800 °C. Two important mass losses at 450 and 700 °C which could be associated to decompositions of portlandite and carbonate of calcium (see DTA) were observed.

The departure of water was decomposed into two domains according to the analysis of Divet et al. [30]:

- Water evaporated to temperatures lower than 450 °C: this water was considered as water weakly linked to the hydrates and, in particular to the calcium-silicates hydrates (C–S–H).
- Water evaporated between 450 and 700 °C: it was considered as strongly bound water.

Beyond 700 °C, Divet et al. [30] considered that the loss was essentially due to the decarbonation.

For an unheated concrete, the mass loss (to temperatures lower than 450 °C) corresponded to the evaporation of free water and water of the C–S–H, ettringite, hydrated monocarboaluminates of calcium [25] and phase present at 400 °C (Brucite or "solid solution of Fe_2O_3") as seen on the DTA. This loss represented about 6% of the initial mass of the sample. The mass loss, at temperatures higher than 450 °C, resulted from the departure of bound water contained in portlandite and C–S–H. This loss was evaluated to about 2.2%.

After thermal treatment, the mass loss, for temperatures lower than 450 °C, decreased. The mass loss becomes very small after a thermal treatment up to 600 °C (only 0.9% of the initial mass of the sample).

4.4. X-ray diffraction

Fig. 14 presents the results obtained by X-ray diffraction on SCC 2 subjected to high temperature.

The X-ray results of unheated concrete (20 °C) revealed the presence of different crystal phases as portlandite, calcite and quartz-α. In our case, we didn't detect ettringite and monosulfoaluminate.

We noticed that the X-ray results of the heated concretes to 150 and 300 °C were very similar to that of unheated concrete. It confirmed that the detected crystal phases did not undergo any transformation at these temperatures (150 and 300 °C).

For higher temperatures, X-ray diffraction confirmed some of the results obtained with DTA. In particular, X-ray results obtained with the concrete heated at 450 and 600 °C did not show the presence of portlandite and Brucite (Fig. 15). Moreover, we did not detect the allotropic transformation of quartz-α to quartz-β for X-ray results at 600 °C, because it is a reversible transformation.

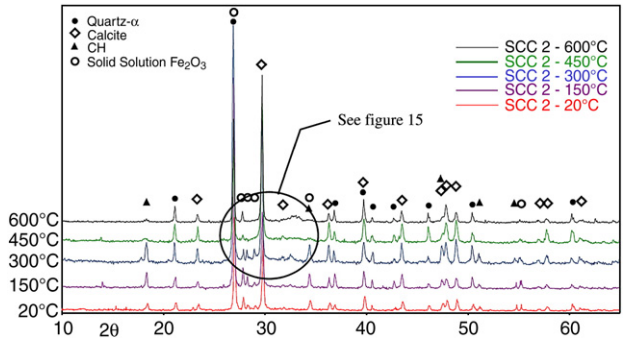

Fig. 14. X-ray diffraction for SCC 2.

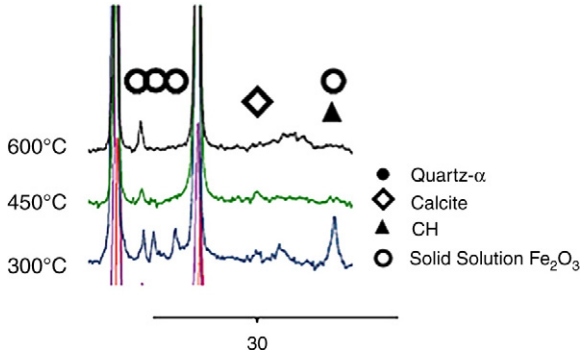

Fig. 15. Zoom on the crystallographic modifications between 300 and 600 °C of Fig. 14.

5. Conclusions

This study concerns the behaviour of SCC subjected to high temperature. The physical and chemical properties and the microstructure after exposure to 150, 300, 450 and 600 °C were studied.

Between 20 and 150 °C, from the microstructural point of view, we did not notice any sensible degradation. We only noticed the departure of bound water contained in C–S–H, and of free water contained in the concrete. These departures of water lead to a slight modification of the porosity.

Between 150 and 300 °C, we observed the first cracks in the concrete, notably within the paste due to the departure of water of different hydrates as C–S–H. These cracks contributed to an increase in porosity. The fraction of anhydrous phases determined by images analysis diminished for the two SCC showing an additional hydration of the anhydrous cement grains. The increase in compressive strength obtained for these two concretes between 150 and 300 °C can therefore be explained by the hydration of anhydrous cement due to the water movements, leading to the formation of hydrates having better bonding properties.

Beyond 300 °C, the microstructure of concrete deteriorated quickly: some chemical transformations took place as the crystal change of the "solid solution Fe_2O_3" or Brucite, the decomposition of the portlandite or the transformation of the quartz-α into quartz-β. All these transformations produced more cracks resulting in an increase in porosity of about 7%.

References

[1] H. Vanwalleghem, H. Blontrock, L. Taerwe, Spalling tests on self-compacting concrete, International RILEM symposium on self-compacting concrete, Proceedings PRO 33 (2003) 855–869.
[2] E. Annerel, L. Taerwe, P. Vandevelde, Assessment of temperature increase and residual strength of SCC after fire exposure, 5th International RILEM Symposium on SCC, 2007, pp. 715–720.
[3] B. Persson, Fire resistance of SCC, Materials and Structures 37 (2004) 575–584.
[4] CERIB, Caractérisation du comportement au feu des Bétons Autoplaçants, Report DT/DCO/2001/29, 2001.
[5] L. Boström, Self-compacting concrete exposed to fire, International RILEM symposium on self-compacting concrete, Proceedings PRO 33 (2003) 863–869.
[6] Étude Feu-Béton, CERIB, ATILH et organisations professionnelles de la construction française (FIB, FFB, FNTP, SNBPE, SYNAD, UNPG), réalisée au CERIB, Rapport final du projet de recherche sur le comportement au feu des bétons, 2006.
[7] H. Fares, A. Noumowé, S. Rémond, Self-consolidating concrete subjected to high temperature: Mechanical and physicochemical properties, Cement and Concrete Research 39 (2009) 1230–1238.
[8] PNBAP, Présentation du projet National de R&D B@P, CD du colloque, Paris, 2006, 21–22 Novembre.
[9] Rilem Technical Committees 129-MHT, Test methods for mechanical properties of concrete at high temperatures, Part 1: Introduction, Part 2: Stress–strain relation,

Part 3: Compressive strength for service and accident conditions, Materials and Structures 28 (181) (1995) 410–414.
[10] D.P. Bentz, P.E. Stutzman, SEM analysis and computer modeling of hydration of Portland cement particles, in: Stark David, Sharon M. DeHayes (Eds.), Petrography of Cementitious Materials, ASTM STP 1215, American Society for Testing and Materials, Philadelphia, 1994, pp. 60–73.
[11] P.E. Stutzman, Scanning electron microscopy imaging of hydraulic cement microstructure, Cement and Concrete Composites 26 (8) (2004) 957–966 Nov.
[12] D.P. Bentz, P.E. Stutzman, C.J. Haecker, S. Rémond, SEM–X-ray imaging of cement-based materials, in: H.S. Pietersen, J.A. Larbi, H.H.A. Janssen (Eds.), Proc. of the 7th Euroseminar on Microscopy Applied to Building Materials, Delft University of Technology, 1999, pp. 457–466.
[13] P.E. Stutzman, J.R. Clifton, Specimen preparation for scanning electron microscopy, in: L. Jany, A. Nisperos (Eds.), Proceedings of the Twenty-First International Conference on Cement Microscopy, 1999, pp. 10–22, Las Vegas, Nevada, April 25–29.
[14] http://rsb.info.nih.gov/nih-image/.
[15] J.J. Friel, X-ray and image analysis in electron microscopy, Gamma-Tech, Princeton, 2003 98 pp.
[16] AFPC-AFREM sur la durabilité des bétons, Méthodes recommandées pour la mesure des grandeurs associées à la durabilité des bétons, INSA-LMDC, Toulouse, 1997 11–12 déc.
[17] X. Liu, Microstructural investigation of Self-compacting concrete and high-Performance concrete during hydration and after exposure to high temperature, Ph-D Thesis, Ghent University, Belgium, 2006.
[18] X. Liu, G. Ye, G. De Schutter, Y. Yuan, L. Taerwe, On the mechanism of polypropylene fibres in preventing fire spalling in self-compacting and high-performance cement paste, Cement and Concrete Research 38 (2008) 487–499.
[19] X. Liu, G. Ye, G. De Schutter, Y. Yuan, Modeling the microstructure change of high performance cement paste at elevated temperature, CONMOD'08, RILEM Proceedings PRO 58 (2008) 439–446.
[20] A. Noumowé, Effet des hautes températures (20–600 °C) sur le béton, Thèse de doctorat, Institut National des Sciences Appliquées, 1995.
[21] G. Platret, Suivi de l'hydratation du ciment et de l'évolution des phases solides dans les bétons par analyse thermique, Caractéristiques microstructurales et propriétés relatives à la durabilité des bétons. Méthodes de mesure et d'essai de laboratoire, Méthode d'essai No. 58, Laboratoire Central des Ponts et Chaussées, Février 2002.
[22] W.P.S. Dias, G.A. Khoury, P.J.E. Sullivan, Mechanical properties of hardened cement paste exposed to temperatures up to 700 °C, ACI Materials Journal 87 (2) (1990) 160–166.
[23] G.A. Khoury, Compressive strength of concrete at high temperature: a reassessment, Magazine of Concrete Research 44 (1992) 291–309.
[24] J.P. Persy, F.X. Deloye, Investigations sur un ouvrage en béton incendié, Bulletin des laboratoires des Ponts et Chaussées 145 (1986) 108–114.
[25] Z.P. Bažant, M.F. Kaplan, Concrete at high temperatures, Longman Addison-Wesley, London, 1996.
[26] E. Nonnet, N. Lequeux, P. Boch, Elastic properties of high alumina cement castables from room temperature to 1600 °C, Journal of the European Ceramic Society 19 (1999) 1575–1583.
Cement and Concrete Research 29 (1999) 1487–1489.
[27] N. Richard, Structure et propriétés élastiques des phases cimentières à base de monoaluminate de calcium, Thèse de doctorat, Paris VI, 1999.
[28] G. Ye, X. Liu, G. De Schutter, L. Taerwe, P. Vandevelde, Phase distribution and microstructural changes of SCC at elevated temperatures, Cement & Concrete Research 37 (2007) 978–987.
[29] W. Sha, E.A. O'Neill, Z. Guo, Differential scanning study of ordinary Portland Cement, Cement and Concrete Research 29 (1999) 1487–1489.
[30] L. Divet, Présentation des techniques de diagnostic de l'état d'un béton soumis à un incendie, Techniques et méthodes des Laboratoires des Ponts et Chaussées, 2005 114pp.